THE ASTROPHYSICAL JOURNAL, 560:445–455, 2001 October 10

A POSSIBLE SOLAR CYCLE DEPENDENCE TO THE HEMISPHERIC PATTERN OF FILAMENT MAGNETIC FIELDS?

D. H. MACKAY
School of Mathematical Sciences, University of St. Andrews, St. Andrews, Fife KY16 9SS, Scotland, UK
AND
A. A. VAN BALLEGOOIJEN
Harvard-Smithsonian Center for Astrophysics, 60 Garden Street, Cambridge, MA 02138
Received 2001 April 17; accepted 2001 May 17

ABSTRACT

The origin of the observed hemispheric pattern of filament magnetic fields is considered. Using a magnetic flux transport model, we simulate the interactions of magnetic bipoles with each other and with polar magnetic fields in the rising and declining phases of the solar activity cycle. In contrast to previous studies, the nonpotential character of the initial coronal fields is taken into account, and the dependence of the hemispheric pattern on the initial tilt and helicity of the bipoles is considered. For the rising phase of the cycle, a range of initial bipole twists and tilt angles can be found that reproduce the observed hemispheric pattern. However, for the declining phase no such range can be found: the predicted fields on the return arms at the rear of switchbacks are consistent with filament observations, but those on the high-latitude east-west arms are not. It is argued that existing observations of the hemispheric pattern are weighted toward the rising phase of the solar activity cycle and may give us a biased view of the Sun. New observations of filament magnetic fields are needed to determine whether there is a cycle dependence of the observed hemispheric pattern.

Subject headings: MHD — Sun: filaments — Sun: magnetic fields

1. INTRODUCTION

For many years it has been known that solar filaments and their birth grounds, filament channels (Martin 1990), have a surprising hemispheric pattern of their chirality: filaments and channels in the northern hemisphere are predominately dextral, while those in the southern hemisphere are predominately sinistral (Leroy, Bommier, & Sahal-Bréchot 1983; Martin, Bilimoria, & Tracadas 1994). Here dextral and sinistral refer to the direction of the *axial* component of the magnetic field (i.e., the component along the filament) as seen by an observer standing on the neighboring, positive-polarity side of the filament channel (Martin, Marquette, & Bilimoria 1992). Martin et al. (1994) based their conclusions on Hα observations of the fine structures of filaments and filament channels on the solar disk, whereas Leroy (1978), Leroy et al. (1983), and Leroy, Bommier, & Sahal-Bréchot (1984) used Hanle measurements of magnetic fields in solar prominences (filaments above the solar limb). The Hanle effect is the only method for determining magnetic fields in polar crown filaments, which obey the hemispheric rule with very few exceptions (Zirker, Leroy, & Gaizauskas 1997a; Bommier & Leroy 1998). The organizational principle behind this hemispheric pattern has not yet been identified.

The flux distributions and observed patterns of prominence magnetic fields are illustrated in Figure 1 for the northern hemisphere. Magnetic flux disperses from decaying active regions and interacts with the polar magnetic field; this produces large areas of unipolar flux that are stretched out by solar differential rotation. This interaction leads to the formation of switchbacks: polarity inversion lines (PILs) that extend from the activity belts to higher latitude and change direction in the east-west sense (see Fig. 1). In the rising phase of the solar activity cycle a PIL confines following polarity flux and is surrounded by leading polarity flux and by the polar fields, which have the same polarity during this period. In contrast, during the declining phase of the cycle a PIL confines leading polarity flux and is surrounded by following polarity flux and polar flux (the polar flux changes sign around the time of cycle maximum). Because switchback PILs follow a different path in both the rising and declining phases of the cycle, it is useful to distinguish different parts of a switchback PIL. In both phases of the cycle a PIL may be split into three distinct sections (Fig. 1). Section (a) is the diagonal part of the lead arm, (b) the east-west section of the lead arm at high latitude, and (c) the return arm near the rear of the switchback. For a single bipole interacting with the polar field in the rising phase there are only sections (a) and (b). Section (c) is absent because there is no flux trailing the active region. Similarly, for the declining phase there are only sections (b) and (c) because there is no flux ahead of the active region. In the declining phase of the cycle sections (b) and (c) are distinct throughout the evolution. In contrast, in the rising phase sections (a) and (b) are only distinct at the start, when the bipole newly emerges. During evolution the two arms quickly align as differential rotation acts on the diagonal part of the lead arm.

Leroy (1978) and Leroy et al. (1983) found that the magnetic fields in prominences along a given switchback (Fig. 1, *arrows with white heads*) are consistent everywhere along that switchback; the axial component of the field is dextral in the north and sinistral in the south. Leroy (1978) comments that "the direction of the field in the polar crown is definitely different from that which would result from the distortion by differential rotation." This is confirmed by recent modeling, which shows that it is difficult to explain the observed hemispheric pattern in terms of surface flux transport effects (van Ballegooijen, Cartledge, & Priest 1998).

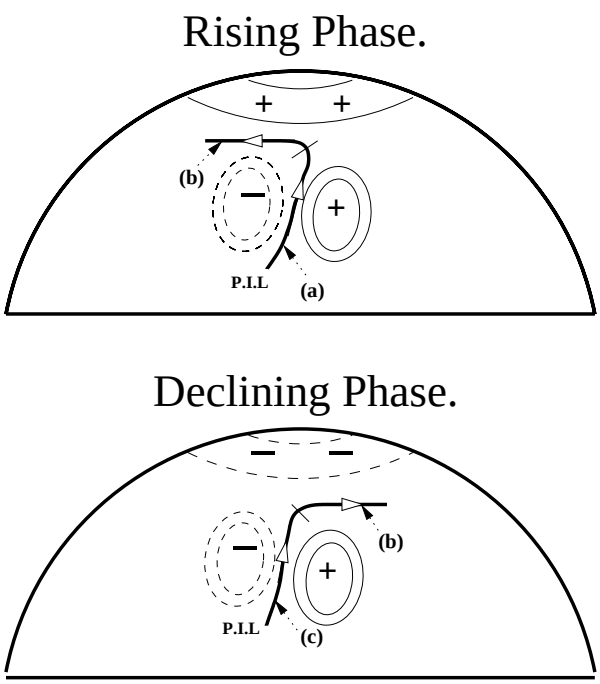

FIG. 1.—Schematic diagram showing the flux distributions and path of the polarity inversion line (PIL) in the northern hemisphere for both the rising and declining phases of the solar cycle. Because of the change in sign of the polar field between the two phases the PIL confines the following flux in the rising phase and the leading flux in the declining phase. Arrows with white heads denote the observed direction of filament magnetic fields. The PIL for each phase may be broken into sections: (*a*) the diagonal part of the lead arm, (*b*) the east-west section of the lead arm at high latitude, and (*c*) the return arm near the rear of the switchback.

The above-mentioned observations have led to the development of new theories of filament channel formation. Some theories use subphotospheric effects to give the correct axial fields in each hemisphere (see, e.g., Rust & Kumar 1994; Priest, van Ballegooijen, & Mackay 1996). Other models use only surface effects to explain the same axial component (Kuperus 1996; Zirker et al. 1997b). At the present time the use of surface effects is preferable, because these effects can be more easily verified through observations. However, it is not clear that the observed hemispheric pattern can indeed be explained this way. Van Ballegooijen et al. (1998) considered whether the surface effects of differential rotation, meridional flows, and diffusion could in fact create the observed axial fields in filaments. By using observed magnetic flux distributions and initial coronal fields that were potential, they simulated the evolution of the photospheric and coronal fields. They found that the above-mentioned surface effects create approximately equal numbers of dextral and sinistral channels in each hemisphere, in contradiction with observations. However, these authors did not take into account the force balance of the coronal plasma, and they only considered statistical relationships between filament chirality and latitude. Van Ballegooijen, Priest, & Mackay (2000) developed a mean field model which properly accounts for the force balance, and Mackay, Gaizauskas, & van Ballegooijen (2000) used this model to compare with observations of specific filaments. In this comparison it was determined that flux transport effects alone, acting on an initial potential field for short periods (27 days), could produce the correct chirality only in about half the cases considered. Slightly better results were obtained when longer terms of evolution (a few months) or the emergence of axial fields through the photosphere were considered. This agreed with the conclusion by van Ballegooijen et al. (1998) that surface effects alone are insufficient to explain the observed hemispheric pattern in filaments.

The purpose of this paper is to use a flux transport model to study the formation of filament channels on the Sun, with the goal of understanding the origin of the observed hemispheric pattern. The model considers the interaction of bipolar flux regions with one another and with the polar fields in both the rising and declining phases of the solar cycle. In contrast to previous studies, we remove the assumption that the corona is initially in a current-free state. Such potential fields are not realistic initial conditions for two reasons. First, new bipoles emerging into the corona are initially not connected to the surrounding fields, i.e., there is a current layer in the corona separating the old and new magnetic flux systems. Second, it is well known that active regions can emerge with positive or negative magnetic helicity (see, e.g., Pevtsov, Canfield, & Metcalf 1995), and such helicity is important in determining the chirality of border filaments (Mackay et al. 1997). Furthermore, we consider the dependence of filament chirality on the tilt of the bipole axis (Tian et al. 1999). Therefore, the present simulations include several new features that are important for understanding the evolution of the coronal field.

This paper is organized as follows. In § 2 the model and initial conditions of the field are described. In § 3 the evolution of a single bipole for both the rising and declining phase of the cycle is given. In § 4 the interaction of multiple bipoles is considered. In § 5 the conclusions are given and present observations discussed. Information requirements from future observational tests of the hemispheric pattern are then put forward.

2. THE MODEL

To simulate the formation of filament channels, we use the magnetic flux transport model of van Ballegooijen et al. (2000). In this model the photospheric magnetic field is acted upon by the flux transport effects of differential rotation, meridional flows, and supergranular diffusion. A spherical coordinate system (r, θ, ϕ) is used, and the magnetic field (B_r, B_θ, B_ϕ) is described in terms of vector potentials. The corona is assumed to be in a force-free state, with electric currents flowing parallel or antiparallel to the magnetic field lines. To obtain such nonlinear, force-free fields, the evolution is carried out using the magnetofrictional method (see, e.g., Yang, Sturrock, & Antiochos 1986). Furthermore, the corona is assumed to evolve according to ideal magnetohydrodynamics (MHD), so that in principle magnetic reconnection occurs only on the photospheric base (in practice, some numerical diffusion occurs throughout the coronal volume). Full details of the numerical method, boundary conditions, and form of differential rotation, meridional flows, and supergranular diffusion can be found in papers by van Ballegooijen et al. (2000) and Mackay et al. (2000).

The purpose of the present paper is to understand how bipolar active regions interact with preexisting coronal fields for different initial helicities and tilt angles. Such interactions are believed to play an important role in the formation of filament channels and filaments on the Sun (Tang 1987). We consider a region in the northern hemisphere

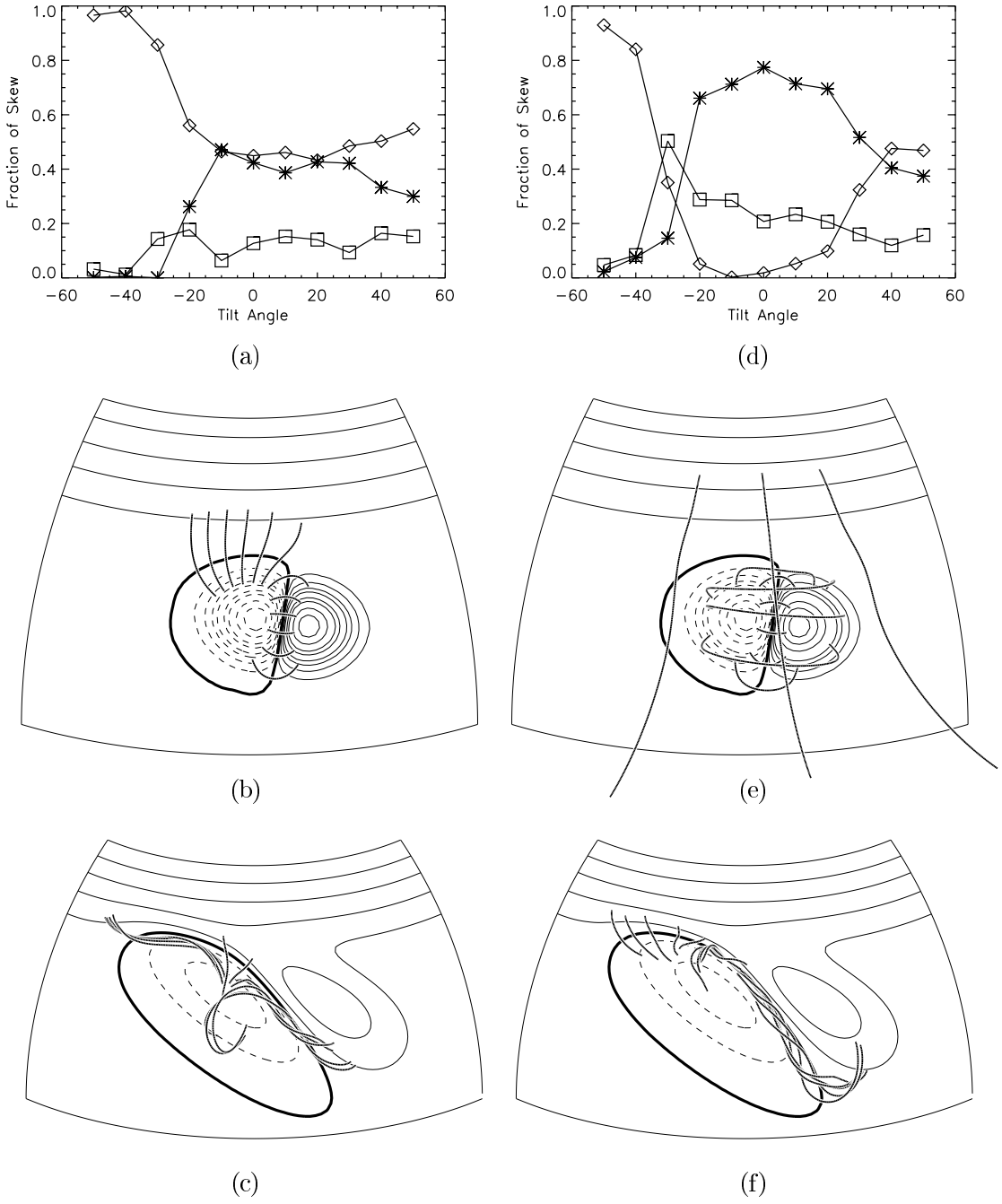

FIG. 2.—Results in the northern hemisphere for a single bipole in the rising phase of the cycle for (*a–c*) an initial potential field and (*d–f*) an independent, untwisted bipole. Graphs (*a*) and (*d*) give the fraction of skew produced along the PIL as a function of the initial tilt angle. Stars represent dextral skew, diamonds sinistral skew, and squares weak skew. Plots (*b*) and (*e*) give the initial field structure for both fields and (*c*) and (*f*) the fields after 54 days of evolution. The longitude range shown in (*b*) and (*e*) is (40, 110), while the range in (*c*) and (*f*) is (20, 110).

with latitude λ ($\equiv \pi/2-\theta$) in the range $0^\circ \leq \lambda \leq 50^\circ$ and longitude in the range $0^\circ \leq \phi \leq 120^\circ$. The computational domain extends from the solar surface ($r = R_\odot$) to a "source surface" at $r = 2.5\ R_\odot$, where the magnetic field is assumed to be radial. Because this volume is in the northern hemisphere, the production of dextral magnetic fields over PILs is required to match the observed hemispheric pattern of filaments. The results can be easily generalized to the southern hemisphere by assuming mirror symmetry with respect to the equatorial plane.

The background field in our model is assumed to be axisymmetric (independent of longitude), representing the polar magnetic field of the Sun. This polar field has a Gaussian profile in latitude such that the peak flux density of ± 10 G occurs at a latitude of 50° and falls off with a $1/e$ width of 10°. To ensure that equatorial diffusion of the polar field is in equilibrium with the poleward meridional flow, the surface flux distribution is initially evolved for a period of 100 days. Then a bipole is emerged into the background field at longitude $\phi_0 = 80^\circ$ and latitude $\lambda_0 = 20^\circ$, using one of the three methods described below. The bipole consists of leader and follower fluxes separated from each other in the direction of solar rotation. The line connecting the centers of leader and follower flux may be tilted relative to the east-west direction by an angle α. The tilt angle lies in the range $-90^\circ \leq \alpha \leq +90^\circ$; positive tilt angles denote a

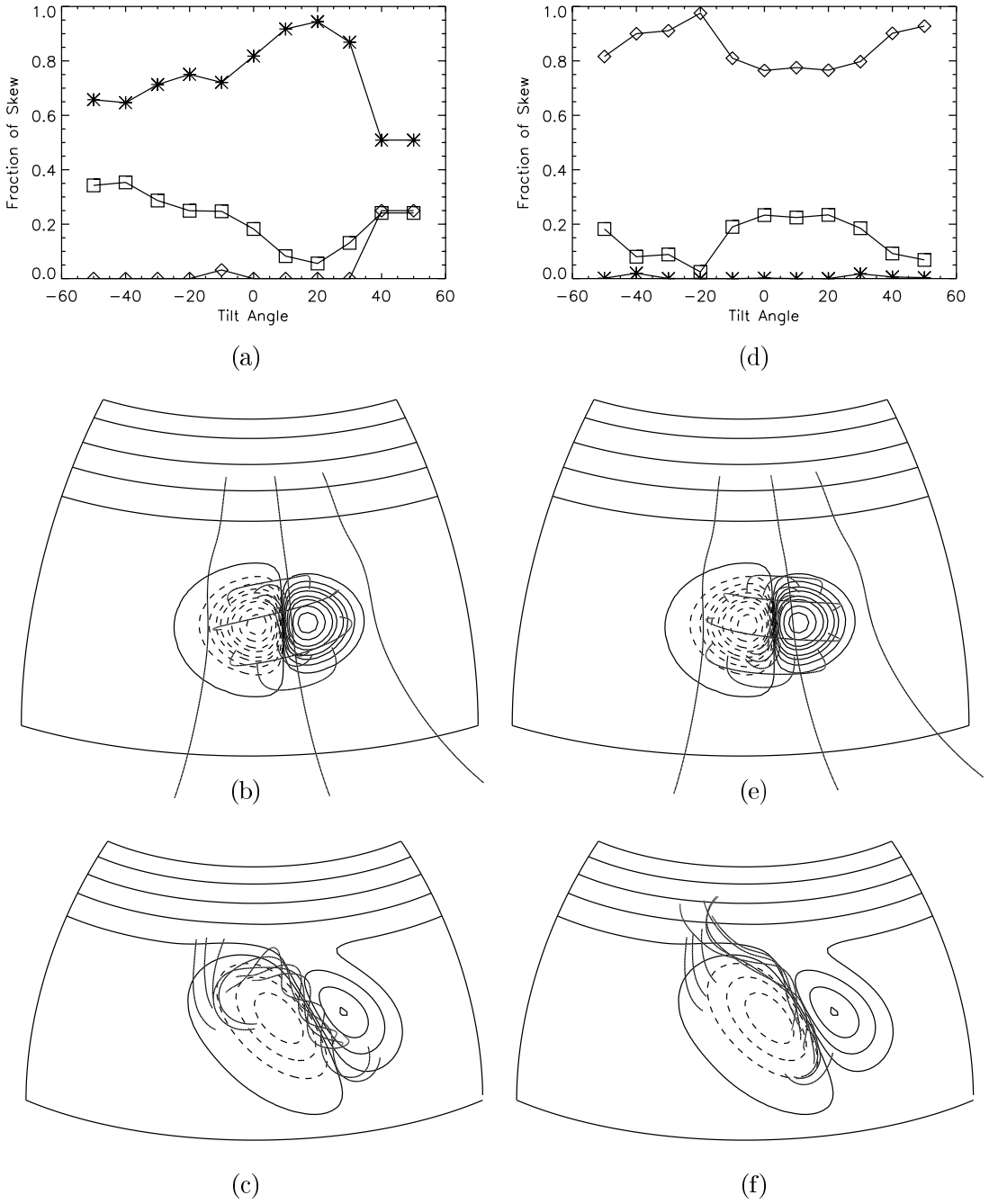

FIG. 3.—Same as Fig. 2, but for (*a–c*) a negatively twisted independent bipole and (*d–f*) a positively twisted independent bipole

leader flux lying equatorward of the follower flux, in agreement with Joy's law. Results obtained by Wang & Sheeley (1989) for cycle 21 and by Tian et al. (1999) for cycle 22 show that roughly 70% of all bipoles on the Sun have positive tilt angles and that 80% of all bipoles have tilt angles in the range -10° to $+30^\circ$. For all simulations presented in this paper the leader flux has positive polarity and the follower flux has negative polarity, which is the correct orientation for bipoles in odd-numbered activity cycles (Hale's law).

To describe the initial magnetic field of the bipole, we introduce a Cartesian coordinate frame (x, y, z) with the origin located on the solar surface ($r = R_\odot$) at longitude ϕ_0 and latitude λ_0. The x- and y-axes are tangential to the solar surface, and the z-axis points radially outward. The x-axis makes an angle α with respect to the east-west direction on the Sun. In this Cartesian reference frame the magnetic field is given by

$$B_x = B_0\, e^{0.5}\left(\frac{z}{\rho_0}\, e^{-\xi} + 4\beta\, \frac{xy}{\rho_0^2}\, e^{-2\xi}\right), \tag{1}$$

$$B_y = 2\beta B_0\, e^{0.5}\left(1 - \frac{x^2 + z^2}{\rho_0^2}\right) e^{-2\xi}, \tag{2}$$

and

$$B_z = B_0\, e^{0.5}\left(-\frac{x}{\rho_0}\, e^{-\xi} + 4\beta\, \frac{yz}{\rho_0^2}\, e^{-2\xi}\right), \tag{3}$$

where $\xi \equiv [(x^2 + z^2)/2 + y^2]/\rho_0^2$, ρ_0 is the half-separation between the peaks of the photospheric flux pattern (corresponding to a heliocentric angle of 5°), B_0 is the peak

flux density ($B_0 = -50$ G), and β is a dimensionless parameter describing the twist of the magnetic field. The above field is axisymmetric with respect to the y-axis and represents a semicircular loop standing vertically above the photosphere.

Three sets of models with different assumptions about the initial condition of the bipole and coronal field are considered. In the first set of models the initial coronal field is assumed to be potential (i.e., current-free). For this configuration, the flux from the bipole [given by $B_z(x, y, 0)$ from eq. (3)] is added to the polar flux, and a potential field is then constructed. The result is shown in Figure 2*b*. In the second set, shown in Figure 2*e*, a potential field is first constructed from the polar flux, and then an untwisted bipole is allowed to emerge into the polar field. The field of the bipole is described by equations (1), (2), and (3) with $\beta = 0$. As the bipole emerges into the corona, it forms a separate magnetic flux system that is initially not connected to the preexisting coronal field; we refer to this as an "independent" bipole. At the interface between the old and new flux systems electric currents exist, so the coronal field for this case is nonpotential (van Ballegooijen et al. 2000). The third type of configuration is an independent bipole with nonzero twist. Figure 3*b* shows a bipole with negative helicity ($\beta < 0$) and dextral skew along the PIL separating the leader and follower fluxes. A case with positive helicity and sinistral skew is shown in Figure 3*e*.

The flux transport effects of differential rotation, meridional flow, and diffusion are allowed to act on the magnetic field for a period of 54 days (2 solar rotations). After 54 days the skew of the field is calculated everywhere along the PIL. The skew is a relevant criterion for determining the dextral/sinistral pattern; Martin & McAllister (1995) found that there is a one-to-one correspondence between the axial magnetic field within filaments and the surrounding corona. The axial magnetic field within a filament points in the same direction as that of the surrounding corona. The skew angle γ is defined as the angle between the magnetic field above the PIL and the horizontal direction perpendicular to the PIL (unit vector pointing from positive to negative polarity). Points with $\gamma > +30^\circ$ are said to have dextral skew, points with $\gamma < -30^\circ$ are assigned sinistral skew, and points with $-30^\circ < \gamma < +30^\circ$ are said to have "weak" skew. In each case the skew is calculated at a height of 10 Mm in the low corona. The type of skew produced by single bipoles in the rising and declining phases of the cycle is described below.

3. SINGLE BIPOLE INTERACTING WITH POLAR FIELD

3.1. *Rising Phase of Activity Cycle*

The interaction of a single bipole with the polar field is now considered for the rising phase of the solar cycle. Figure 2*a* shows the results for an initial potential field after 54 days of evolution. The fraction of the PIL that has dextral (*stars*), sinistral (*diamonds*), and weak skew (*squares*) is plotted as a function of the initial tilt α of the bipole axis. All three types of skew are obtained, but the amount of skew of each type depends on the initial tilt of the bipole. No hemispheric pattern of dextral skew is found. In the range of -10° to $+30^\circ$ roughly equal amounts of dextral and sinistral skew are produced, while at extreme tilt angles sinistral skew becomes the more dominant. This results agrees with the earlier simulations by van Ballegooijen et al. (1998), who were also unable to reproduce the observed hemispheric pattern from an initial potential field. Over the entire range of tilt angles there is a preference for sinistral skew, which is the wrong type for the northern hemisphere.

Figure 2*d* shows the corresponding graph for an independent untwisted bipole that has emerged within the polar field. In this case there is a range of tilt angles for which dextral skew is by far the most dominant. For these tilt angles (-20° to $+30^\circ$) anywhere from 60% to 80% of the PIL skew is dextral, with roughly 20% weak skew but hardly any sinistral. At the extreme tilt angles the lengths of sinistral and dextral skew are comparable (for $\alpha > +30^\circ$) or sinistral skew is dominant ($\alpha < -30^\circ$). Therefore, when an independent untwisted bipole is evolved, there is an optimal range of bipole tilt angles that reproduces the observed hemispheric pattern. This range covers the dominant tilt angles observed on the Sun (-10° to $+30^\circ$; see Tian et al. 1999).

From Figures 2*a* and 2*d* it is clear that different configurations of the initial coronal magnetic field produce very different results. To illustrate why this is the case, we now consider a bipole with a tilt angle of $+10^\circ$. Figure 2*b* shows the initial configuration for a potential field, and Figure 2*c* shows the evolved field after 54 days. Note that in Figure 2*b* there are strong connections between the polar field and the follower flux of the bipole. The solid lines at the photosphere represent positive flux, the dashed lines negative flux. The thick bold line represents the PIL, and the lines connecting positive and negative flux denote the field lines. For both the diagonal part of the lead arm and east-west section of the switchback the field lines pass over the PIL with little or no skew. On the diagonal part of the lead arm, which lies mainly north-south, the field lines are east-west. On the east-west section at high latitude the field lines are mainly north-south. After the field lines have been evolved for 54 days (Fig. 2*c*), a strong skew develops along the entire length of the PIL, dextral along the diagonal part and sinistral on the east-west. The sinistral skew results from differential rotation acting on field lines that were initially north-south. In contrast, the dextral skew on the diagonal part results from differential rotation rotating the PIL counterclockwise while the arcades remain nearly east-west. This builds up a dextral axial component, which is localized and maintained along the PIL by flux cancellation (van Ballegooijen & Martens 1989). For an initial potential coronal field equal amounts of dextral and sinistral skew are always produced with no hemispheric pattern because of the initial orientation of the arcades on the diagonal and east-west parts of the lead arm.

Figure 2*e* shows the initial configuration for an independent untwisted bipole, and Figure 2*f* shows the corresponding field after 54 days. Because the bipole is initially isolated from the polar field, all the flux in the bipole connects in an east-west direction, and there are no longer any north-south connections. The differential rotation acting on the bipole produces dextral skew along the diagonal part of the lead arm. However, along the east-west section of the PIL the follower flux cancels the polar flux, and connections are made between the polar field and bipole. These connections have a dextral skew because of the initial east-west connectivity of the bipole. Therefore, the dextral skew is able to progress much farther along the PIL and to higher latitudes than in the previous case (compare Figs. 2*f* and 2*c*). This is a result of the orientation of the bipole relative to the polar

field. It plays a major role in producing an axial component (dextral) that matches the observed hemispheric pattern.

The effect of adding a twist to the field of the bipole is now considered. To begin with, negative values of the twist parameter β are considered. Negative values are chosen because the observations by Pevtsov et al. (1995) and others have shown that negative helicity dominates for active regions in the northern hemisphere. Figure 3*a* shows the fraction of skew produced after 54 days of evolution as a function of the tilt angle α for $\beta = -0.6$. It can be seen that the initial helicity strongly affects the results, because dextral skew is now by far the most dominant type over all tilt angles. There is practically no sinistral skew, but a reasonable amount of weak skew at the extreme angles. Similar results were found for $\beta = -0.3$ and -0.9. Therefore, by adding negative twist to the bipoles a skew consistent with the hemispheric pattern of filaments is produced.

Figure 3*b* shows the initial magnetic field for a tilt angle of 0° and $\beta = -0.6$. Note that the effect of this negative helicity is to produce a natural dextral skew along the diagonal portion of the lead arm at low heights. Figure 3*c* shows the field lines overlying the PIL after just 27 days of evolution. An inverse-S–shaped structure is produced, consistent with X-ray observations of the corona using the *Yohkoh* satellite (see, e.g., Rust & Kumar 1996). At all points along the PIL the axial component points to the right. The reason for the difference between Figures 3*c* and 2*c* is that the initial twist gives a preferred direction along the PIL at the start. As the PIL rotates counterclockwise the axial component on the diagonal part of the lead arm is able to propagate much faster up the PIL onto the east-west section. This preferred direction counters the effect of differential rotation on the east-west section and produces a dextral structure along its entire length.

The simulations are now repeated, but this time positive helicity is added to the bipole ($\beta = +0.6$). This produces a sinistral skew within the initial field of the bipole (Fig. 3*e*). After the field has been evolved for 54 days sinistral skew is the most dominant (Fig. 3*d*). Similar results were found for $\beta = +0.3$ and $+0.9$. The resulting field line structure after 27 days can be seen in Figure 3*f*. This model produces the wrong chirality for the northern hemisphere, but one should keep in mind that only a minority of the active regions in the northern hemisphere have positive helicity.

3.2. *Declining Phase of Activity Cycle*

A single bipole interacting with the polar field is now considered for the declining phase of the solar cycle. In Figure 4*a* the fraction of skew produced as a function of the tilt angle can be seen for the potential field. As expected, after 54 days of evolution there is no hemispheric pattern of dextral skew. Between the tilt angles of $-30°$ and $+10°$ roughly equal amounts of dextral and sinistral skew are produced. However, outside this range sinistral skew is the most dominant. In Figure 4*b* the corresponding results are shown for the untwisted bipole. Surprisingly, this time no

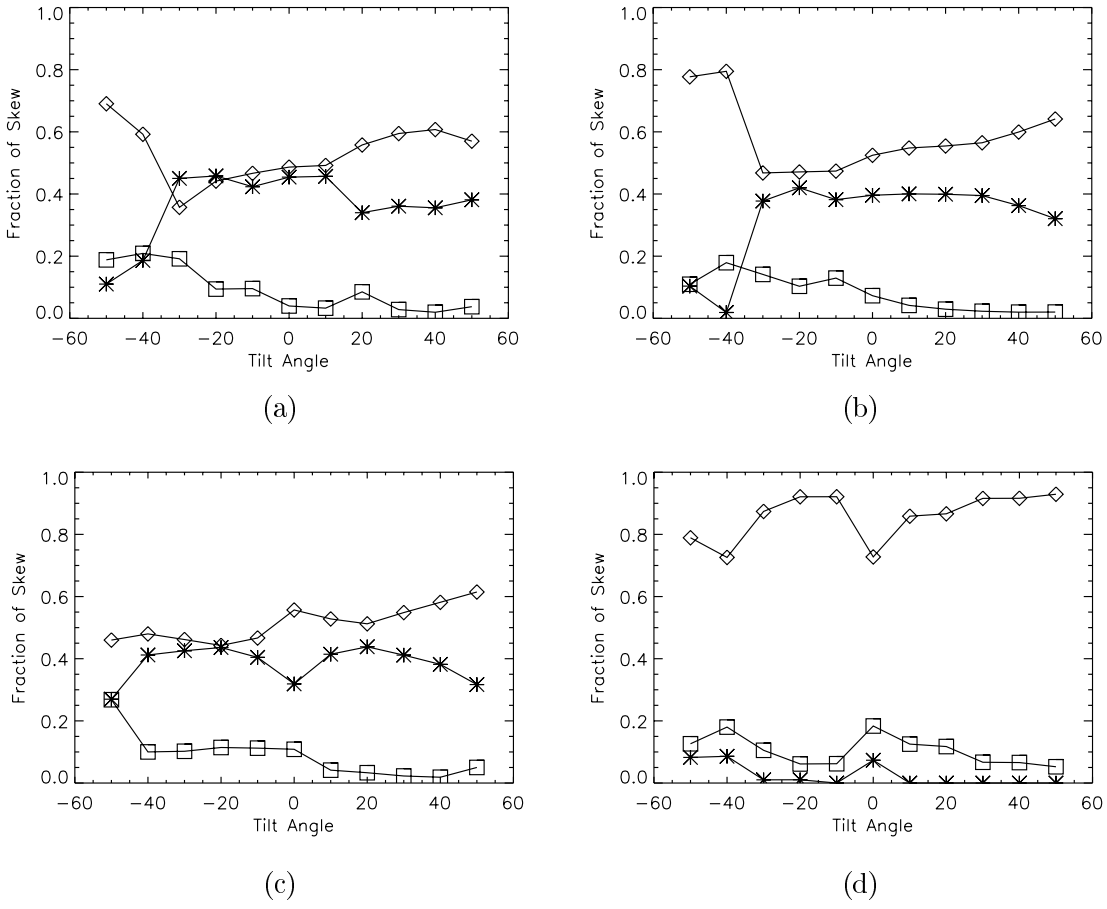

FIG. 4.—Fraction of skew produced along the PIL in the northern hemisphere by a single bipole in the declining phase of the cycle for (*a*) an initial potential field, (*b*) an independent, untwisted bipole, (*c*) a negatively twisted independent bipole, and (*d*) a positively twisted independent bipole. Stars represent dextral skew, diamonds sinistral skew, and the squares weak skew.

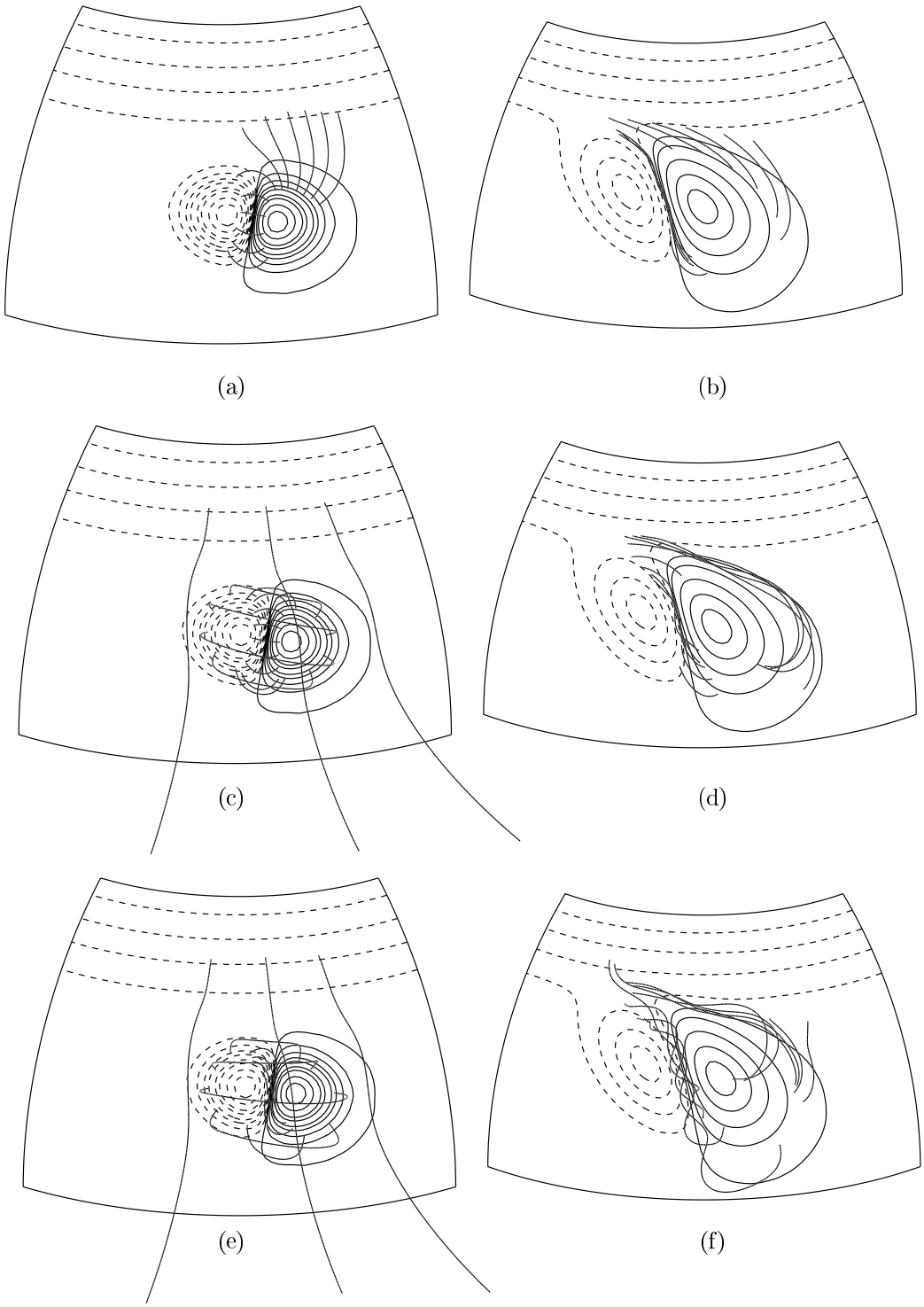

FIG. 5.—Field line structure in the declining phase for single bipoles in the northern hemisphere for (*a*) an initial potential field and (*b*) the field evolved for 27 days. Similar plots are shown in (*c*) and (*d*) for an independent untwisted bipole and in (*e*) and (*f*) for a negatively twisted independent bipole. The longitude range in (*a*), (*c*), and (*e*) is (40, 110), while the range in (*b*), (*d*), and (*f*) is (20, 110).

hemispheric pattern of dextral skew is found, even though one was found for the rising phase. In fact, having an independent bipole now makes the field more sinistral than having an initial potential field. Even when negative helicity is added to the bipole (Fig. 4*c*; $\beta = -0.6$) the correct hemispheric pattern cannot be reproduced, and only equal amounts of dextral and sinistral skew are formed. Adding positive helicity (Fig. 4*d*; $\beta = +0.6$) yields dominantly sinistral fields, which is incorrect for the northern hemisphere.

From these simulations it can be seen that very different results are obtained in the declining phase of the cycle than in the rising phase. In the declining phase no hemispheric pattern that matches the observations can be produced, even when helicity that should give the correct axial component is added. In fact, the declining phase of the cycle in the northern hemisphere seems to prefer the formation of sinistral skew rather than dextral. The converse would be true for the southern hemisphere.

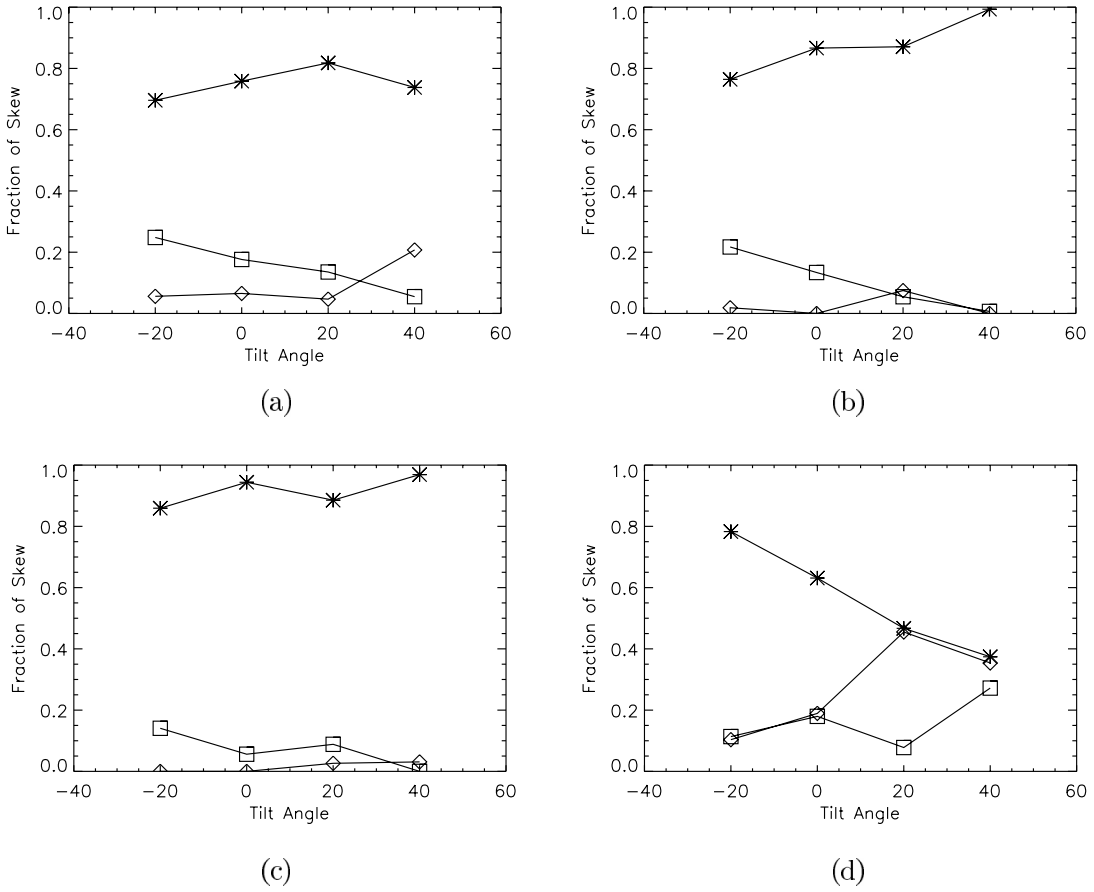

FIG. 6.—Fraction of skew produced along the PIL as two bipoles interact in the northern hemisphere in the rising phase of the cycle for (*a*) a potential field, (*b*) two untwisted bipoles, (*c*) two negatively twisted bipoles, and (*d*) two positively twisted bipoles. Stars represent dextral skew, diamonds sinistral skew, and squares weak skew.

A consideration of the evolution of the field lines will show why the declining phase of the cycle prefers the formation of sinistrally skewed field lines in the northern hemisphere. To begin with, the potential field configuration is considered. In Figure 5*a* the initial configuration can be seen and in Figure 5*b* the evolved field after 27 days. In the initial configuration the field lines on the return arm lie east-west, and on the east-west section of the lead arm they are north-south. As described above, a dextral skew is formed on the return arm and sinistral skew is formed on the lead arm (Fig. 5*b*).

However, if an independent, untwisted bipole is considered, the type of skew formed does not change. In Figure 5*c* the initial configuration is shown, where all the leader flux of the bipole connects to the follower flux. In contrast to the rising phase, this now produces a sinistral field along the east-west section of the lead arm. As the flux diffuses out and interacts with the polar field, the initial east-west component of magnetic field along the lead arm is maintained, and a sinistral axial component is produced (Fig. 5*d*). Therefore, the feature that helped us produce the correct axial component in the rising phase of the cycle now produces the wrong component because of the different path of the PIL. In fact, it produces a sinistral skew stronger than that of the potential field. A dextral skew can only form along the return arm.

Even when negative helicity is added to the bipole, similar results are found (Figs. 5*e* and 5*f*; $\beta = -0.6$). This is because the east-west component of the field within the bipole dominates its interaction with the overlying polar field, and the twist within the bipole plays only a minor role. Therefore, along the lead arm of the switchback there is a natural tendency to produce sinistral skew. In fact, the only way we have been able to overcome this natural tendency is to inject oppositely directed axial fields from below the photosphere. To produce a dextral field along this section of the PIL, the axial flux emergence has to break up the existing connections between the leader and follower fluxes within the bipole. However, the simulations by van Ballegooijen et al. (2000) and Mackay et al. (2000) have shown that the required rate of axial flux emergence is much larger than observed. Hence, axial flux emergence does not appear to be a viable explanation for the observed hemispheric pattern during the declining phase of the cycle.

In summary, we find that with a single bipole the observed hemispheric pattern can be easily reproduced in the rising phase of the solar cycle, but not in the declining phase. We now consider multiple bipoles.

4. MULTIPLE BIPOLES INTERACTING WITH THE POLAR FIELD

The simulations are now repeated, but this time the interaction of two bipoles is considered. The interaction is followed for both the rising and declining phases of the solar

cycle. The size of the computational domain is increased in the ϕ-direction ($0° \leq \phi \leq 150°$), and the bipoles are located at longitudes $\phi_1 = 80°$ and $\phi_2 = 110°$. The skew is calculated only along that part of the PIL where the two bipoles interact with each other, because this part was not considered in the previous simulations.

In Figure 6 the fraction of different types of skew produced after 54 days of evolution in the rising phase can be seen as a function of the tilt angle of the bipole. Both bipoles are taken to have the same tilt angle. The results are shown for a potential field (Fig. 6*a*), two untwisted bipoles ($\beta = 0$; Fig. 6*b*), two negatively twisted bipoles ($\beta = -0.6$; Fig. 6*c*), and two positively twisted bipoles ($\beta = +0.6$; Fig. 6*d*). When the independent bipoles are considered, they are independent from each other and from the polar field. From the graphs it is clear that the most predominant type of skew formed as the bipoles interact is dextral. However, in the positive-helicity case equal amounts of dextral and sinistral skew can be formed for some tilt angles. Therefore, again in the rising phase of the solar cycle, if untwisted bipoles or negative-helicity twists are considered, an axial component that matches the hemispheric pattern can be easily produced.

The production of the dextral axial component is now considered. In Figure 7*a* the initial configuration for the potential field is shown. Along the location where the two bipoles interact the PIL lies mainly north-south and the arcades east-west. The field configuration is similar to that inside the bipole, and as the PIL is rotated counterclockwise by differential rotation, a dextral axial component is produced (Fig. 7*b*).

However, if the bipoles emerge into the background field, the configuration is very different, because there are initially no connections between the bipoles. The field between the bipoles is that of the polar field (Fig. 7*c*). The polar field runs north-south and produces a natural axial component along the PIL separating the two bipoles. To an observer standing on the (positive) leading flux of the trailing bipole and looking toward the trailing flux of the leading bipole, the axial component is dextral. As the bipoles diffuse out and connections are made between them, the direction of the polar field is maintained (Fig. 7*d*). Therefore, the type of chirality produced depends on the direction of the polar field that lies between the two bipoles. For the rising phase this will yield a dextral field consistent with the observed hemispheric pattern. Adding helicity to the bipoles only changes the results slightly, because the dominant field is still that due to the polar field.

The simulations are now repeated, but for the declining phase of the solar cycle. The results are shown for the potential field (Fig. 8*a*), two untwisted bipoles ($\beta = 0.0$; Fig. 8*b*), two negative helicity bipoles ($\beta = -0.6$; Fig. 8*c*), and two positive helicity bipoles ($\beta = +0.6$; Fig. 8*d*), again for the northern hemisphere. From the graphs it is clear that sinistral skew is the most dominant and that the axial component does not match the observed hemispheric pattern. Sinistral skew is dominant because the polar field has reversed sign and points south-north (Fig. 9*c*). Therefore, exactly the opposite situation to that shown in Figures 7*c* and 7*d* is found. Now, to an observer standing on the positive-polarity side of the second bipole, the field points to the left and is sinistral. As with the single bipole, it is found that the declining phase of the solar cycle prefers the formation of sinistral skew rather than dextral.

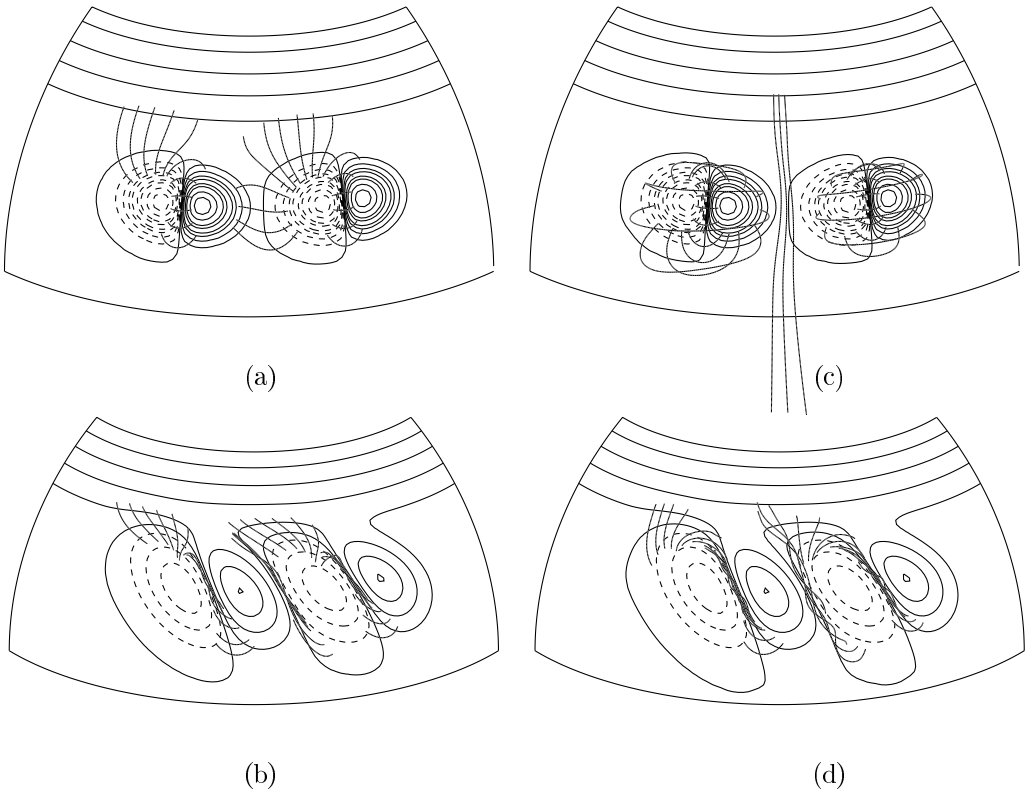

FIG. 7.—Field line structure in the rising phase for two bipoles interacting in the northern hemisphere for (*a*) an initial potential field and (*b*) the field evolved for 27 days. Plots (*c*) and (*d*) show the same, but for independent untwisted bipoles. The longitude range in (*a*) and (*c*) is (45, 140), while the range in (*b*) and (*d*) is (30, 140).

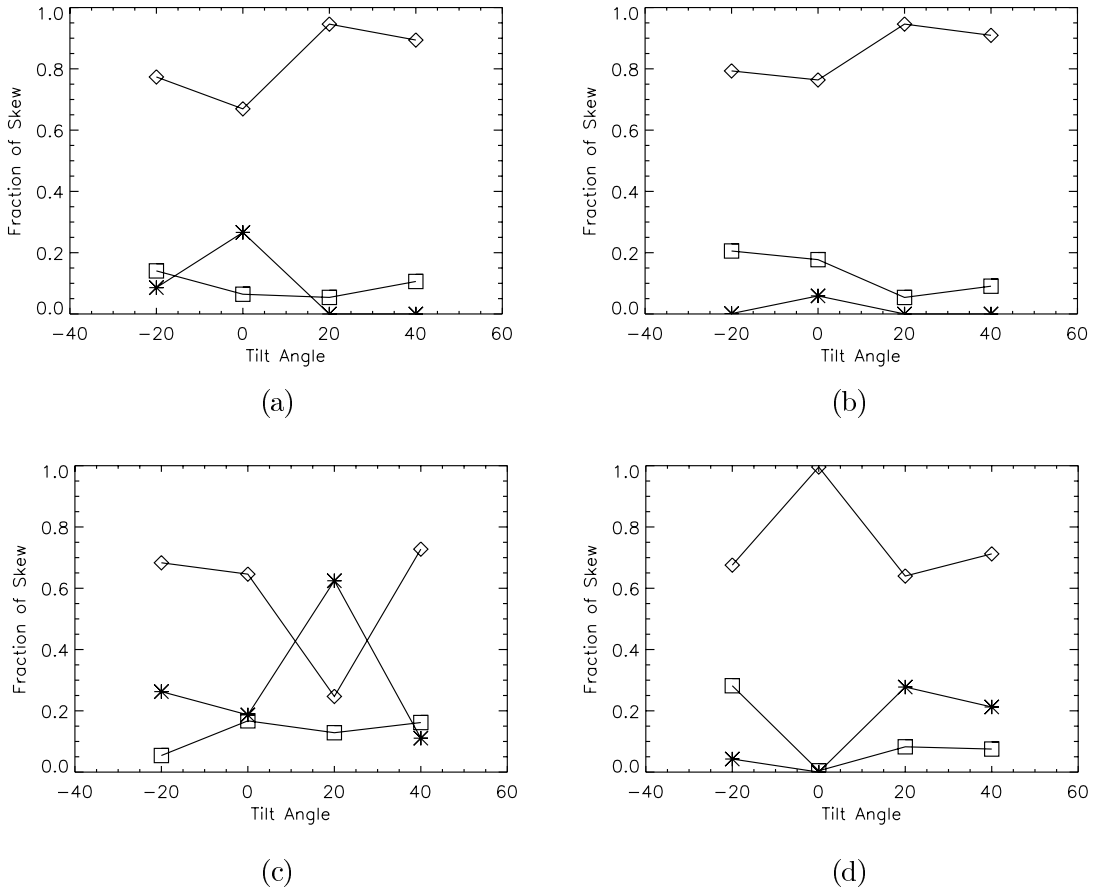

FIG. 8.—Same as Fig. 6, but for the declining phase of the cycle

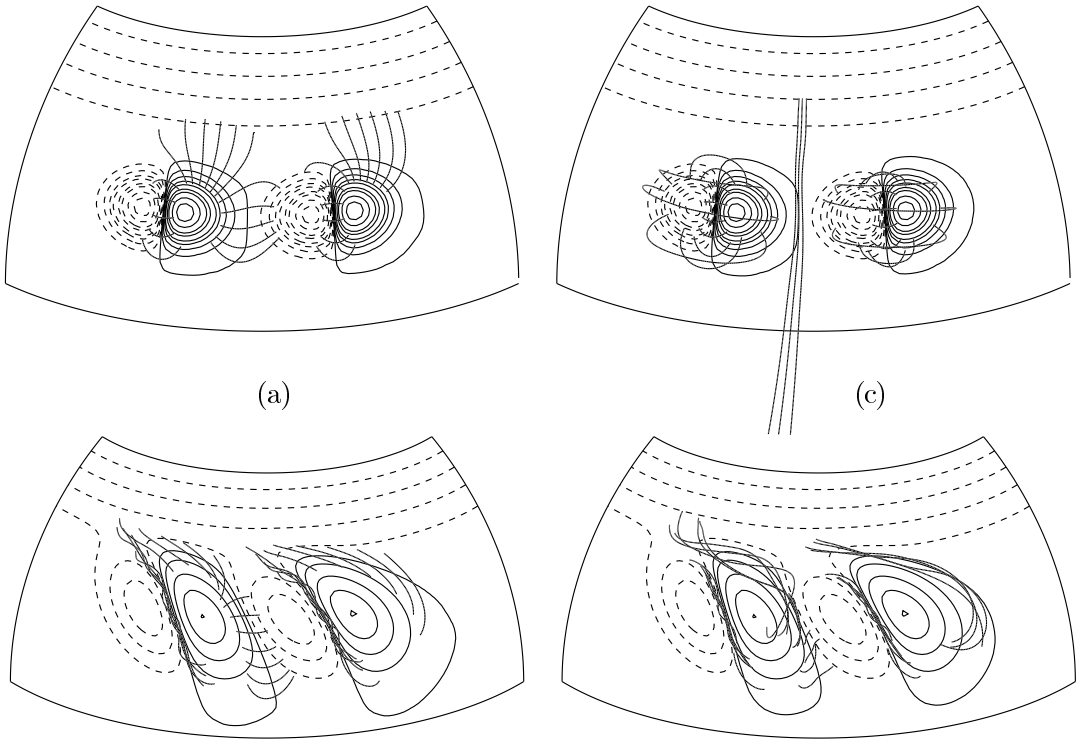

FIG. 9.—Same as Fig. 7, but for the declining phase of the cycle

5. CONCLUSIONS

A systematic survey of the way in which bipoles interact with one another and with polar fields has been carried out. The survey aimed to determine the origin of the hemispheric pattern of axial components within filaments. In contrast to previous simulations, more realistic initial coronal fields have been considered. These coronal fields take the form of newly emerged bipoles independent of the surrounding polar field. The bipole could be untwisted or have a positive or negative twist. The use of independent bipoles removed the restrictive assumption that the initial coronal field was potential. This allowed the inclusion of essential new physics into the simulations. This more realistic initial configuration with coronal currents gave results more consistent with observations than those from an initial potential field. The simulations were conducted in the northern hemisphere, but the results can be easily generalized to the southern. This showed that the hemispheric pattern could be easily reproduced in the rising phase of the solar cycle, but not in the declining phase.

For the rising phase the hemispheric pattern was reproduced for both single and multiple independent bipoles. For a single, untwisted bipole there was a range of tilt angles ($-20°$ to $+30°$), consistent with the observed tilt angles (Wang & Sheeley 1989; Tian et al. 1999), that gave the correct axial component. Furthermore, if the bipole was twisted with the dominant sign of helicity for each hemisphere, then the hemispheric pattern could be reproduced over all relevant tilt angles. For multiple independent bipoles the correct axial component after interaction was due to the direction of the initial polar field that lay between them. In the rising phase this polar field always pointed in the direction matching the hemispheric pattern.

In contrast, for the declining phase of the solar cycle no definite hemispheric pattern could be reproduced. For a single bipole the type of axial component obtained depended very much on which part of the PIL was being considered. On the lower latitude return arm the correct axial component could be reproduced, but on the higher latitude east-west lead arm the wrong axial component was produced. Even the addition of helicity of the correct sign for each hemisphere gave the same result without a definite hemispheric pattern. This was a natural consequence of the orientation of the field inside the bipole, which was very difficult to overcome. For multiple bipoles interacting with each other the wrong axial component was obtained because the polar field between the two bipoles had the wrong direction.

The simulations above show a clear distinction between the rising and declining phases of the solar cycle. In the rising phase it is relatively easy to reproduce the correct axial component, but in the declining phase it is not. The simulations also show a clear distinction between the east-west lead arm and return arm of the PIL in the declining phase. Because there seems to be a clear distinction between the rising and declining phases, the observations of the hemispheric pattern are now discussed. Martin et al. (1994) used three separate data sets: the first contains 82 filaments and covers the period 1989 May–1990 July; the other two contain 72 filaments and cover the periods 1991 August 30–September 30 and 1992 June 8–20 (an exact breakdown of numbers of filaments for these data sets is not given). It is clear that the first data set lies in the rising phase of the cycle, the second one lies at solar maximum, and the third lies in the declining phase. Therefore, it appears that the data sets of Martin et al. (1994) are weighted toward the rising phase, whereas our simulations agree with the observed hemispheric pattern.

In addition to the data sets of Martin et al. (1994), an independent data set of Hanle effect measurements made within 296 prominences exists (Leroy et al. 1984). The data set covers the period 1974–1982 and shows the same hemispheric pattern (Bommier & Leroy 1998) as Martin et al. (1994). An exact breakdown of dates of filament observations is not available in the literature; however, it is clear that the Leroy data sets are also weighted toward the rising phase of the cycle (1975–1980), where the modeling suggests that there should be a hemispheric pattern.

To clarify this issue and verify that the hemispheric pattern indeed exists in both rising and declining phases of the solar activity cycle, new measurements of prominence magnetic fields are needed. Such measurements should include polar crown filaments. Detailed information about the location and chirality of each filament needs to be recorded. Without such information it is impossible to determine whether existing models are consistent with the observations or not. Future modeling should focus on specific observed filaments and should use the observed photospheric magnetic fields. Mackay et al. (2000) made a first step in that direction, but in order to resolve the important questions about filament channel formation, more detailed observational inputs will be required.

Financial support for the work was given by the UK Particle Physics and Astronomy Research Council. The numerical simulations were carried out on the PPARC-funded Compaq MHD Cluster in St. Andrews. Support for the collaboration of the authors was provided by NSF Grant ATM 98-08063 to Helio Research Corporation, La Crescenta, California.

REFERENCES

Bommier, V., & Leroy, J.-L. 1998, in ASP Conf. Ser. 150, New Perspectives on Solar Prominences, ed. D. Webb, D. Rust, & B. Schmieder (San Francisco: ASP), 434
Kuperus, M. 1996, Sol. Phys., 169, 349
Leroy, J.-L. 1978, A&A, 64, 247
Leroy, J.-L., Bommier, V., & Sahal-Bréchot, S. 1983, Sol. Phys., 83, 135
———. 1984, A&A, 131, 33
Mackay, D. H., Gaizauskas, V., Rickard, G. J., & Priest, E. R. 1997, ApJ, 486, 534
Mackay, D. H., Gaizauskas, V., & van Ballegooijen, A. A. 2000, ApJ, 544, 1122
Martin, S. F. 1990, in IAU Colloq. 117, Dynamics of Quiescent Prominences, ed. V. Ruždjak & E. Tandberg-Hanssen (Lecture Notes in Physics 363; New York: Springer), 1
Martin, S. F., Bilimoria, R., & Tracadas, P. W. 1994, in Solar Surface Magnetism, ed. R. J. Rutten & C. J. Schrijver (NATO ASI Ser. C, 433; Dordrecht: Kluwer), 303
Martin, S. F., Marquette, W. H., & Bilimoria, R. 1992, in ASP Conf. Ser. 27, The Solar Cycle, ed. K. L. Harvey (San Francisco: ASP), 53
Martin, S. F., & McAllister, A. H. 1995, BAAS, 27, 961
Pevtsov, A. A., Canfield, R. C., & Metcalf, T. R. 1995, ApJ, 440, L109
Priest, E. R., van Ballegooijen, A. A., & Mackay, D. H. 1996, ApJ, 460, 530
Rust, D. M., & Kumar, A. 1994, Sol. Phys., 155, 69
———. 1996, ApJ, 464, L199
Tang, F. 1987, Sol. Phys., 107, 233
Tian, L., Zhang, H., Tong, Y., & Jing, H. 1999, Sol. Phys., 189, 305
van Ballegooijen, A. A., Cartledge, N. P., & Priest, E. R. 1998, ApJ, 501, 866
van Ballegooijen, A. A., & Martens, P. C. H. 1989, ApJ, 343, 971
van Ballegooijen, A. A., Priest, E. R., & Mackay, D. H. 2000, ApJ, 539, 983
Wang, Y.-M., & Sheeley, N. R., Jr. 1989, Sol. Phys., 124, 81
Yang, W. H., Sturrock, P. A., & Antiochos, S. K. 1986, ApJ, 309, 383
Zirker, J. B., Leroy, J.-L., & Gaizauskas, V. 1997a, Sol. Phys., 176, 279
Zirker, J. B., Martin, S. F., Harvey, K, & Gaizauskas, V. 1997b, Sol. Phys., 175, 27